Advanced Engineering Informatics 46 (2020) 101180

Contents lists available at ScienceDirect

Advanced Engineering Informatics

journal homepage: www.elsevier.com/locate/aei

A CNN-based personalized system for attention detection in wayfinding tasks

Yanchao Wang [a], Yangming Shi [b], Jing Du [b], Yingzi Lin [a], Qi Wang [a,*]

[a] Northeastern University, 360 Huntington Ave, Boston, MA 02115, United States
[b] University of Florida, 460F Weil Hall, Gainesville, FL 32611, United States

ARTICLE INFO

Keywords:
Wayfinding task
Virtual reality (VR)
Electroencephalography
Deep neural network
Convolutional neural networks
Attention detection

ABSTRACT

Firefighters are often exposed to extensive wayfinding information in various formats owing to the increasing complexity of the built environment. Because of the individual differences in processing assorted types of information, a personalized cognition-driven intelligent system is necessary to reduce the cognitive load and improve the performance in the wayfinding tasks. However, the mixed and multi-dimensional information during the wayfinding tasks bring severe challenges to intelligent systems in detecting and nowcasting the attention of users. In this research, a virtual wayfinding experiment is designed to simulate the human response when subjects are memorizing or recalling different wayfinding information. Convolutional neural networks (CNNs) are designed for automated attention detection based on the power spectrum density of electroencephalography (EEG) data collected during the experiment. The performance of the personalized model and the generalized model are compared and the result shows a personalized CNN is a powerful classifier in detecting the attention of users with high accuracy and efficiency. The study thus will serve a foundation to support the future development of personalized cognition-driven intelligent systems.

1. Introduction

Firefighters work in extreme situations and perform psychologically-demanding tasks [1,2]. According to a report from the National Fire Protection Association (NFPA), there were 58,835 firefighter injuries in 2017, and 42 percent of the incidents occurred at the fire ground [3]. The National Institute of Occupational Safety and Health (NIOSH) discovered that disorientation is one of the most common causes of firefighter fatalities [4]. In an investigation of the disorientation challenge of firefighters in the U.S. from 1979 to 2001, prolonged zero visibility conditions, which is caused by heavy smoke conditions lasting for more than 15 minutes, occurred in 100% of the cases [5]. According to [6], besides the influence imposed by the heavy smoke on spatial visibility, high smoke density could severely reduce the speed of human movements and the capability of information processing [7]. In such conditions, because of the lack of affordable and reliable indoor localization systems [8], memorized information turns into the main source to perform wayfinding tasks.

However, firefighters have to take in a large amount of information in a short time [9], which adds tremendous cognitive load to them. As a result, memorization becomes a critical skill for firefighters to navigate and even retreat from the fire ground. Additionally, firefighters have varying capabilities in dealing with different types of information owing to the individual differences in prior knowledge and other intellectual skills [10]. Thus, apart from monitoring firefighters' overall cognitive load, it is crucial to identify what kind of information they are memorizing or recalling. Such knowledge will lead to effective intervention strategies in necessary conditions to help them better focus on processing demanding information in their preferred format.

There is limited knowledge on the connection between the format of wayfinding information and its influence on the cognitive system of individuals despite its importance. The lack of understanding of the connection constrains us from identifying what kind of information is being memorized or recalled when massive input is given to a firefighter. As a result, firefighters might have to process information that they are not proficient in, which could further risk their safety and the successes of tasks.

One of the most pressing challenges related to any cognition-driven intelligent system is the difficulty of detecting and predicting selective attention focus, i.e., what information a person is paying attention to

* Corresponding author.
E-mail addresses: wang.yanch@husky.neu.edu (Y. Wang), shiyangming@ufl.edu (Y. Shi), eric.du@essie.ufl.edu (J. Du), yi.lin@northeastern.edu (Y. Lin), q.wang@northeastern.edu (Q. Wang).

https://doi.org/10.1016/j.aei.2020.101180
Received 1 May 2020; Received in revised form 25 August 2020; Accepted 17 September 2020
Available online 5 October 2020
1474-0346/

and processing at a certain time point. In a highly dynamic environment, information stimuli of different types and formats are usually mixed, such as mixed phonological, visual, spatial, and other sensory cues. Although physiological measures including eye-tracking are effective in detecting what a person is “looking at”, they usually fail to tell what the person is “seeing” and “digesting”. In aviation research, researchers use a verbalization approach for intent and attention identification, where the test subjects are required to verbalize what they are thinking [11,12], but it is often done in a controlled laboratory environment and lacks efficiency. In addition, self-reporting is yet another cognitive process that may interrupt the information processing of the cognitive process under investigation. As a result, there is a pressing need for an approach to automatically detect the specific information type and format a person is processing when information stimuli are mixed and thus difficult to separate.

To bridge the knowledge gaps listed above, this study designs a set of virtual wayfinding tasks, including both memorizing period and performing period in four scenarios. We use neural activities for automated attention detection based on the presumption that the EEG data shows identifiable patterns when a person views and processes a certain type of information. As a result, the selective attention focus is detectable by examining the strength of each representative EEG pattern. Without losing the generality of the findings, this paper focuses on different wayfinding information types, including landmarks, routes, and survey information. Then, we implement the convolutional neural networks (CNN) to identify what type of information is being memorized or recalled. Particularly, we build a personalized model and a generalized model to differentiate which groups of models are more capable of detecting the connections between attentions and information.

2. Literature review/background

2.1. Wayfinding information

Literature shows that spatial knowledge determines individuals’ wayfinding behaviors and strategies [13]. Spatial knowledge can be categorized into three main stages, landmark knowledge, route knowledge, and survey knowledge [14]. Landmark knowledge is the knowledge of a specific location in an environment which is identified and memorized based on its shape, size, color, and contextual information [15]. Route knowledge is the knowledge of memorizing a fixed sequence of locations that will be experienced during the journey [16]. Survey knowledge corresponds to the information which integrates sequences and knowledge from different experiences [14]. In [13], landmark knowledge, route knowledge, and survey knowledge are illustrated as the knowledge about a point in space, the knowledge about a sequence of points, and the knowledge about an area respectively. Cognitive science literature has discovered the relationship between spatial knowledge acquisition strategies and spatial memory development effectiveness in navigation tasks [17–22].

With the development of virtual reality technologies, more and more researchers started to use an VR-based environment to investigate individuals’ wayfinding behavior and have confirmed its efficacy [6,23,24]. They found that VR technology can provide a fidelitous virtual environment to arouse an individual’s mental process and evoke their behavioral responses to the simulated virtual emergencies with high ecological validity [24–26]. For example, [25] explored the influence of repeated exposures and mental stress on human wayfinding performance using virtual reality. They found that the simulated fire emergency scenarios negatively affected participants’ wayfinding performance, but the repeated exposure diminished the negative impact of the simulated fire emergency scenarios. In addition, [27] used another VR-based virtual environment to investigate the influence of crowd flow on human evacuation behavior during building fire emergencies. They created a virtual metro station and a number of characters (NPC) to simulate the fire emergency scenario. The experiment was conducted in Beijing, Los Angeles, and London. They confirmed that a VR-based experiment is an effective method for studying human evacuation behavior. They also found that the uneven splits of crowd flow motivated participants to follow the majority of the crowd during indoor evacuation and participants from different have similar evacuation behavior. [28] also confirmed the effectiveness of the VR-based environment in earthquake drills. They developed an immersive earthquake emergency scenario in a hospital and used the Verbal Protocol Analysis (VPA) to investigate an individual’s decision-making process. They found that participants tended to be influenced by other people and wanted to accompany with other people during the evacuation. In summary, the previous studies revealed that VR can provide an effective environment to investigate an individual’s evacuation and wayfinding behavior in the indoor building environment. In addition to the LRS model, some researchers have started to investigate the role of attention in human wayfinding decision-making process. [29] found that eye movement is associated with the forward motion and turning during the navigation. The eye movement may represent an individual’s decision-making process during wayfinding. [30] also found that an individual’s review attention has correlated with final wayfinding and task performance during building inspections. However, previous studies have done little to investigate how brain activities affected visual attention related to wayfinding performance. Therefore, we used the VR-based environment integrated with an EEG device to address this knowledge gap.

2.2. EEG and deep learning based analysis

Electroencephalography (EEG) is a widely used neuroimaging technique that measures the summation of electric fields produced by pyramidal neurons in the cortical layers of the brain [31]. EEG has an outstanding time-domain resolution for the rapid propagation speed of electric fields, especially in imaging large scale brain activity [32]. However, the propagation of electric fields from the source to the sensor is influenced by the tissues, which results in the fact that the signal of EEG channels is often highly spatially correlated and at a low signal-to-noise ratio [31]. Despite the drawbacks of EEG, it has many applications in neuroscience and psychology, including measuring the level of fatigue [33], mental workload [34,35], and emotions [36]. Additionally, EEG is widely used as a sensor to collect brain activity as the input of brain-computer-interfaces (BCI)[37].

Processing EEG data has been a difficult task. In recent years, deep learning methods have been extended to the existing EEG processing methods, especially in the field of classification of EEG data. Among all the methods, convolutional neural networks (CNN) have been the choice of the algorithm in most EEG research since 2015 [31]. The choice is not only driven by its success in other fields such as computer vision [38], but also by its capabilities in learning without any prior feature selections and exploiting hierarchical structure from the data [39]. For example, in [40], a pyramidal one-dimensional CNN is proposed for automated epilepsy detection with an accuracy of around 99.1%. In [41], CNN is used as a feature extraction tool and proven to outperform other feature extraction neural networks such as artificial neural networks and recurrent neural networks in recognizing Schizophrenia. To predict driver’s cognitive states, a channel-wise convolutional neural network is designed and achieved robust and improved performance over conventional methods [42]. Additionally, CNN is used in [43] to deal with the mental workload level classification problem.

The input to the neural network varies and there is no consensus which input can achieve the best results in understanding the cognitive load using EEG data. Researches have achieved promising results using the raw EEG data as the input [44,45]. However, feature extraction is still an effective way to deal with the non-stationarity, low signal-to-noise ratio, and non-linearity of raw EEG signals [43]. Additionally, the power spectrum density (PSD) of classical frequency bands are widely adopted by the EEG community as one of the most important features of EEG data [31]. Thus, the time-frequency domain obtained via a short-time Fourier transform (STFT) is often used as input to neural networks [43,46,47].

In summary, current literature has provided limited knowledge on the connection between the stimuli of wayfinding information and the reaction of the human brain. Also, there is a knowledge gap in choosing the proper input to the CNN model to classify the attention of the subject. To address these issues, we selected CNN as the classifier with the PSD acquired by STFT as the input. Multiple CNN models are built to explore a good CNN structure with decent accuracy and high training speed.

The rest of the paper is arranged as follows. In Section 3, the wayfinding experiment is proposed and data from 20 subjects are collected. The data is analyzed in Section 4 to validate the importance of building a personalized model for the identification of the kind of information and whether it is being memorized or recalled. Two groups of CNN models are built and the test results are presented in Section 5. The result is further be discussed in Section 6 along with the limitation of this research and future work.

3. Experiment

3.1. Participants

Twenty subjects aging from 20 to 28 (mean = 24.6) were recruited for this study. The participants included 5 females and 15 males. All of them were reported to have sufficient literacy levels in English and no health issues related to computer gaming. 7 out of 20 have some VR experiences before and 13 of them play video games with an average of 5.63 h per week. Each participant was informed of the purpose and procedures of the experiment before the experiment started.

3.2. Tasks

The experiment contains four scenarios based on the wayfinding literature: a control group, a landmark group, a route group, and a survey group. And the spatial information provided to the groups except the control one is shown in Fig. 1.

In the control group, subjects are asked to find targets without any prior given spatial information. In the landmark group, a sequence of landmarks is presented to participants in the format of both images and texts. The route group represents a series of relative directions. In the survey group, the map of the maze is provided with the information on their initial point, initial direction, and the location of three targets. Information of different groups was given before participants entering the maze, and they had three minutes to memorize the information. The maze was built in Unity software® and the texture is set to be underground as Fig. 2.

In every scenario, subjects were asked to start from a start point with a mark on the ground to find three targets sequentially in the maze with one type of information. We developed a virtual maze workflow to randomly generate maze models using the external library [48] and Software Development Kit (SDK) in Unity 3D. To ensure the same difficulty of the maze models, several algorithms were used in this workflow. First, we created several maze components as the predefined prefabs in the maze generation pool including different types of rooms, start room, end room, and different types of corridors. Then, the system randomly picks each maze component without repeating between the mazes. Second, we used the Bowyer-Watson algorithm to perform Delaunay Triangulation for all the picked maze components. The purpose is to fully connect all the picked maze components. Third, we utilized a Prim Algorithm to calculate the minimum spanning tree for the fully connected maze components. Forth, we applied a 15% possibility to connect the leaf for the minimum spanning tree and then we used the A* algorithm to find the shortest path from the start room to the end room. At last, the system fully connects all the maze components with

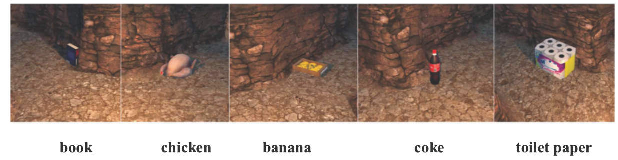

(a) Landmark group information (from start point to target A)

Left, right, left, right, left, left, right, left, right

(b) Route group information (from start point to target A)

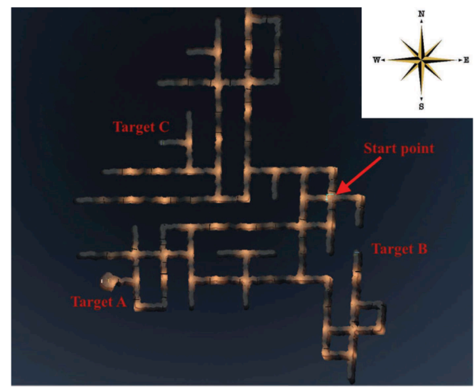

(c) Survey group information

Fig. 1. Example of spatial information.

Fig. 2. Underground maze environment.

the corridor components. Before each maze generation, we could define the shortest distance from the start room to the end room to ensure that each maze model maintains the same level of difficulty.

3.3. Procedure

The procedure of the experiment contained six parts. First, after reading and signing the informed consent, participants were asked to answer a background questionnaire about their genders, ages, occupations, and experiences on video games and virtual reality. The participants also reported their abilities in understanding various kinds of spatial knowledge in the questionnaire. Then, cube comparison test and shape memory test [49] were taken to measure participants' capabilities in maintaining spatial orientation and their ability in memorizing shape, location, and orientation in provided materials. Third, subjects were instructed with their tasks in the maze and the control of the game. Because the EEG device used in this experiment is sensitive to body movement, despite the wide application of virtual reality in the wayfinding research area [25,50], in this experiment, a monitor was selected as the display of the environment, and mouse and keyboard were chosen for subjects to control the direction of sight and the movement on the screen. Thirty minutes were provided for each individual to get familiar with the control and the environment of the game in a training scenario that has the same texture but different maze layout with other scenarios used for experiments. After the training, four wayfinding tasks were performed and the EEG signals are collected by the Enobio 32 from Neuroelectrics® with the frequency at 500 Hz during the procedure. The environment and setup of the experiment are shown in Fig. 3.

In every wayfinding task, a one-minute baseline will be recorded, three minutes will be given for them to memorize the certain type of information, and six minutes will be provided for subjects to move in the maze and find targets in sequence with the help of the memory of given information. NASA Task Load Index (NASA-TLX) questionnaire is taken as an objective measurement of the mental demand, physical demand, temporal demand, overall performance, effort, and frustration level on users after each task. The Control group will be taken as the first group and the sequence of the rest of tasks will be shuffled randomly before the experiment. After the four tasks, subjects will be interviewed about their used strategies and opinions about the experiment, such as how they memorize information, how much information they can memorize in each task, and what type of information helps them in the task.

3.4. Pre-processing on EEG

Because brain activity signal is often buried by noises from environment and body activities in raw EEG signals, which are called "artifacts" [31], pre-processing methods are ought to be used to acquire the clean brain activity signal from the raw EEG signal.

We used EEGLAB, an open-source toolbox for Matlab [51], to preprocess the raw EEG signal. First, the EEG data were downsampled from 500 Hz to 250 Hz. Then, a bandpass filter with low cut-off frequency at 1 Hz and the high cut-off frequency at 120 Hz was applied to remove the potential impact on the further process from high-frequency noise [43]. PREP-pipeline [52] was used to detrend the signal. At last, independent component analysis (ICA) [53] and ADJUST [54] were utilized in collaboration to separate and reject artifacts automatically, especially noises generated by muscles and eye movements.

After acquiring the clean EEG data, short-time Fourier transform (STFT) using the Hanning window with the length at 250 samples and overlapping length at 50 samples was implemented on EEG data to get the power spectrum density (PSD) of the brain activity. The frequency domain energy data was further separated into eight sub-bands, delta (1–4 Hz), theta (4–7 Hz), lower alpha (8–10 Hz), upper alpha (10–12 Hz), lower beta (13–15 Hz), upper beta (14–30 Hz), lower gamma (30–45 Hz), and upper gamma (65–120 Hz) [55,56].

Fig. 3. Experiment environment with EEG.

4. Data analysis

PSD data which include 32 channels and, for each individual channel, 8 sub-bands ranging from 1 Hz to 120 Hz are visualized using violin plots for individuals to investigate into different brain activities exposed to different types of information and tasks from different subjects in this section. In violin plots, only the data in the first three minutes of the performing period is chosen to ensure the balance of the data set size between the performing period and the memorizing period. The y-axis represents decibels of the amplitude relative to that in the baseline, and the x-axis shows the performing period and memorizing period in four different groups. Subject 2 and subject 21 are selected as examples to demonstrate the differences between individuals. The PSD of channels in the prefrontal, and parietal cortex, which are understood to be related to attention and working memory [57] are compared in the rest of this section.

$$Amplitude_{dB} = 20 \cdot log_{10}\left(\frac{|Amplitude|}{|Amplitude_{Base}|}\right) \quad (1)$$

According to [58], an increase in the theta-band energy in the frontoparietal network is related to memory encoding and retrieving performance. Similar results could also be observed in the prefrontal and temporal-parietal regions [59]. It is reported that the right part has a higher theta amplitude than the left part in encoding visual information [59]. C3 and C4 are selected as two representative channels in the areas mentioned above. Fig. 4 shows the theta-band energy in the C3 channel which is on the left region mentioned above. Also, the theta-band energy on the right part could be represented by the C4 channel is plotted in Fig. 5.

Observing the violin plots of the two channels, for both subjects, theta-band energy in C3 and C4 channels has increased in average in the performing period of the control group comparing to the baseline. Subject 2 has a slight increase in average theta-band energy in both channels from the baseline when the subject is handling the landmark memorizing, landmark performing, route performing, and survey performing tasks. Also, subject 21 is reported to have a higher theta amplitude in the landmark and route information memorizing stage in two channels. This shows that when subjects were trying to memorize or recall information in these two tasks the cognitive load increased in most of the cases. Additionally, comparing C3 and C4 of subject 21, it could be found that the theta amplitude in the right region is higher than that in the left region when the subject is performing in the landmark, route, and survey group according to the result of Wilcoxon signed-rank test. It indicates that the subject 21 was encoding visual information during the performing period and does not fully rely on the information provided. However, apart from the coherence of the literature mentioned above, violin plots also show a slight decrease in theta amplitude in average in C3 and C4 when the subject 2 was memorizing route and survey knowledge according to the baseline. A similar decrease could be observed when the subject 21 was performing in the landmark group in C3 and survey group in both channels. This shows that some kind of information does not stimulate much cognitive load in C3 and C4 channels for some subjects.

In [60], the cognitively demanding task activates the central-executive network which includes the dorsolateral prefrontal cortex, and posterior parietal cortex. The posterior parietal cortex has a complex

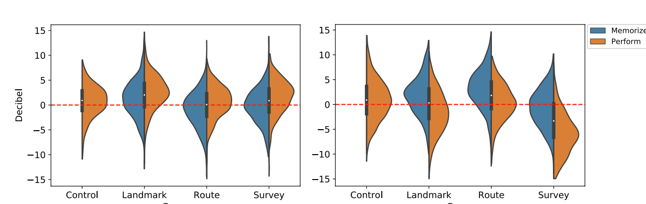

Fig. 4. C3 channel theta band of subject 2 (left) and subject 21 (right).

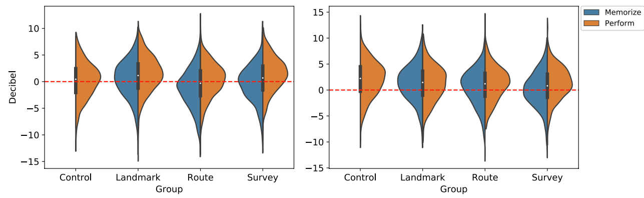

Fig. 5. C4 Channel theta band of subject 2 (left) and subject 21 (right).

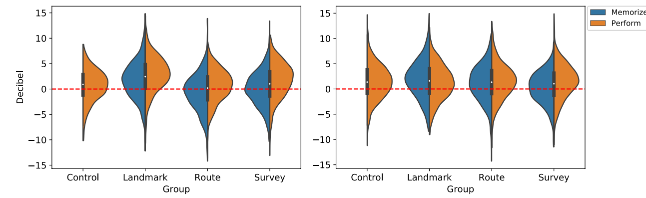

Fig. 7. F3 Channel theta band of subject 2 (left) and subject 21 (right).

ability to perceive and react to stimuli in the visual field [61]. In other words, it coordinates both eye-gazing point and hand movement in space to accomplish the interaction to the real world.

P3 channel is selected to be the representative of the posterior parietal cortex and the violin plot shows the theta band of P3 in Fig. 6. According to the literature, P3 is expected to have higher theta-band energy during the performing period than the baseline and memorizing period because of the activation of the posterior parietal cortex. For both subjects, participants in the control group and the landmark group showed higher theta-band energy than that in the baseline. Additionally, the performing period given the survey knowledge activates the posterior parietal cortex more than the baseline and memorizing period. However, a similar pattern could not be observed in the landmark group and the route group of two subjects.

Dorsolateral prefrontal cortex is another crucial component of the central-executive network [60] which plays a maintenance role in working memory, especially under high loads [62]. Because channel F3 is located in the dorsolateral prefrontal cortex, the theta-band energy is plotted in Fig. 7.

According to the figures, it could be observed that for both subjects, the dorsolateral prefrontal cortex is activated during all circumstances except the memorizing period of the route knowledge for subject 2 in average.

In summary, according to the analysis above, the theta energy measured during the performing part in the control group is slightly above the baseline for two subjects in all visualized channels in the prefrontal, and parietal cortex. Additionally, among all the memorizing periods in three groups of subject 2, there is more theta energy in the prefrontal and parietal cortex given landmark information than that in other groups. It shows that memorizing landmark information brings more mental workload for subject 2 than other groups. A similar conclusion could be made among performing periods of subject 2. Moreover, except for the right side of the prefrontal and temporal-parietal region, the landmark information brings the most mental workload to subject 2. Also, we find that on average the route group information brings the least amount of mental workload both in memorizing and performing. However, for subject 21, route information brings more mental workload in the left prefrontal and temporal-parietal region than that in the posterior parietal cortex, and the dorsolateral prefrontal cortex. Comparing the theta energy between memorizing and performing, it could be found that, in the left prefrontal and temporal-parietal region, the performing period stimulated more theta frequency energy in subject 2, but it brought less theta-band energy in subject 21. The PSD of the remaining 18 subjects are included in Fig. S.1. Comparing the mental workload stimulated by the same task on four brain regions in subjects, individual differences become a factor

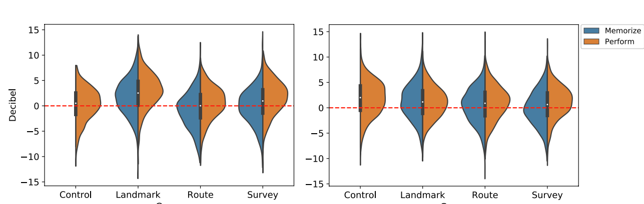

Fig. 6. P3 Channel theta band of subject 2 (left) and subject 21 (right).

that could not be ignored in analyzing the mental workload introduced by various types of information. Thus, as a result, it is necessary to try the individual-level model in classifying what kind of information is influencing the subject and if the subject is encoding or decoding the information. Moreover, to deal with the existence of the large variance and poor separation, neural networks are selected to be the classification method in further analysis.

5. Convolutional neural network

As what has been discussed in the Section 2.2, CNN is selected as the classifier of the PSD data acquired from EEG signals.

5.1. Major components of CNN

5.1.1. Convolutional layer

Convolutional (Conv) layer plays an essential feature learning role in the CNN architecture. Each Conv layer consists of one set of learnable kernels with a receptive kernel field smaller than the input size in width and height but equal in depth. During the forward pass, each kernel convolves along the width and the height of the input signal. In other words, it calculates the dot product between the kernel and the local region input at all positions and adds a bias. After the kernel slides over the width and the height, a 2-D activation map will be produced. The output of the Conv layer is derived by stacking every activation map generated by kernels in the Conv layer along with the depth. As is shown in Fig. 8.

5.1.2. ReLU layer

To increase the nonlinearity of the network and without affecting the receptive field of the convolutional layer, an activation function is usually implemented after a Conv layer. There are many commonly used activation functions, for example, the sigmoid function $\sigma(x) = (1 + e^{-x})^{-1}$, the hyperbolic tangent $f(x) = tanh(x)$, and the rectified linear unit (ReLU) $f(x) = max(0, x)$. In this paper, the ReLU is selected to be the activation function in the neural network for its speed and minimum penalty on accuracy.

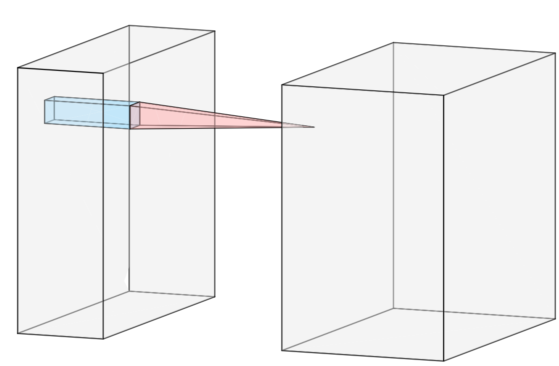

Fig. 8. Convolutional layer, two grey cuboids represent input and output tensors of the convolutional layer, and the blue cuboid is the kernel corresponding to one layer of activation map.

5.1.3. Pooling layer

To reduce the spatial size of output from the Conv layer to reduce the computational load, and to avoid overfitting at the same time, a pooling layer is placed periodically among a set of Conv layers. The pooling layer separates every slice of the input into rectangles with the same shape and no overlaps, and output the maximum or the average, depending on the pooling layer function selection. The output of this layer will have a lower size in height and width but keep the depth unchanged.

5.1.4. Fully-connected layer

In a fully-connected layer, each neuron is connected to all of the elements in the output from the previous layer. Thus, the calculation in this layer could be considered as multiplying the input by a weight matrix and adding a bias vector. It is used as the final part of CNN to connect features extracted through the Conv layer, ReLU layer, and pooling layer to the target output.

5.1.5. Input and labels

Because the PSD for every second contains energy amplitude of 32 channels and 8 sub-bands, it could be viewed as a digitized one-channel image in the shape of 32×8 pixels as shown in Fig. 9.

After acquiring the energy of 8 sub-bands in 32 channels using STFT for every second, the PSD is formatted into an $1 \times 32 \times 8$ tensor and further stacked as a time series with a label of the task the participant was working on. As shown in the illustration of tasks in Section 3, the EEG data could be labeled into seven categories of tasks, the performing part in four groups, and the memorizing part in the landmark group, route group, and survey group.

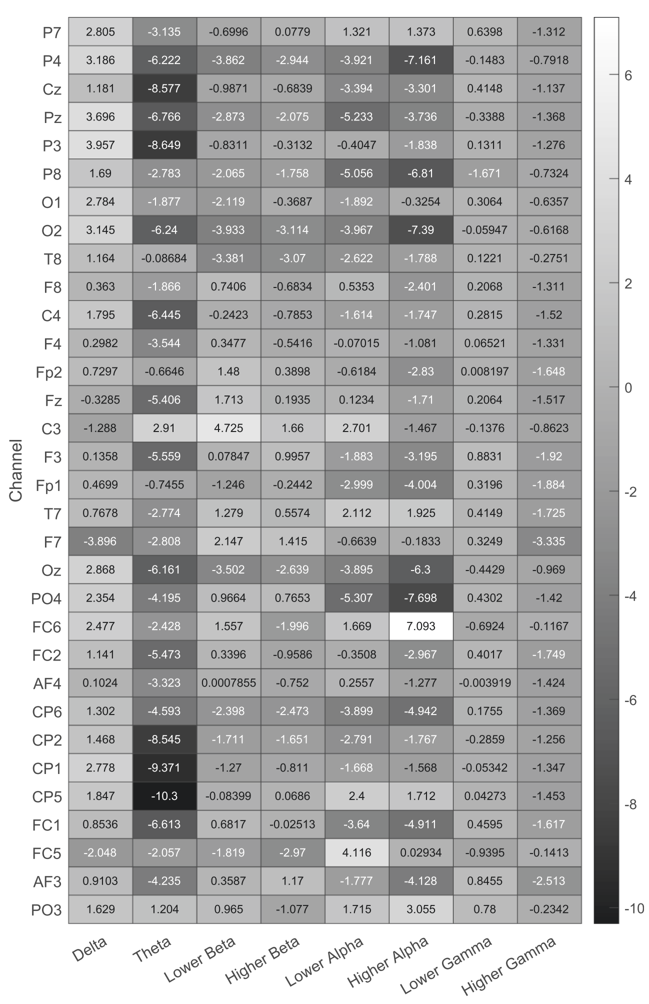

Fig. 9. Image of PSD.

5.2. Personalized model

Due to the individual differences of activated brain regions among participants, we first designed a personalized model that is coherent with the idea of a personalized information system. The purpose of this model is to build a personalized CNN based on each individual's own EEG data, and, as a result, the model could neglect the effect of individual differences and deal with personalized behavior.10-fold cross-validation is applied to compare personalized CNN models. Among the 6,300 samples acquired for each individual, there are 900 PSDs for each category of task. The CNN is trained by 5,670 samples in each iteration, and the rest 630 samples are saved for evaluating the accuracy of the model.

In order to find the optimal structure of neural network for the wayfinding task classification problem, two candidate convolutional neural networks (CNN1 and CNN2) are proposed and the structural parameters of neural networks are provided in Table 1. In the table, Conv1 represents the convolutional layer with 1 input channel and 8 output channels. Its kernel size is selected to be 5 and the stride is 1. And the Conv2 represents the convolutional layer with 8 input channels and 16 output channels. Zero paddings for Conv1 and Conv2 are set to 2 to ensure the size of the output to be suitable input for the next layer. All convolutional layers use ReLU as the activation function for introducing nonlinearity to the neural network, and batch normalization is applied after each convolutional layer to improve the stability of the neural network. The Pool 2×2 is the 2D max pooling layer with kernel size as 2×2, strides for the height and width as 2, and no padding applied. The number in the FC Layer column means the output size of a fully-connected layer. The loss function is the cross-entropy loss and the optimizer is selected to be the Adam optimizer [63] with the learning rate at 0.01.

Taking CNN2 as an example, the structure of the neural network is designed as Fig. 10. In the figure, the input to the network is a $1 \times 32 \times 8$ tensor acquired from the result of STFT. After the first convolutional layer Conv1, the second convolutional layer Conv2 was added, followed by a pooling layer for down-sampling to reduce the number of parameters and computational load. Then, fully-connected layers are added for feature extraction and the output is an array with 7 elements. The matrix is further processed by the soft-max function which determines probabilities for all classes and outputs the corresponding digit of the label with the highest probability.

5.3. Generalized model

To further investigate the possibility of a generalized model, convolutional neural networks have been trained by the data collected from 19 subjects. 10-fold cross-validation is also applied in quantifying the accuracy of the generalized model. In the training procedure, 119,700 samples from 19 subjects are separated into a training set that includes 90% of data. The trained CNN is further tested by the remaining 10% data in evaluating the performance. The 6,300 PSDs from the remaining subject is saved to test if the generalized model could still accurately classify the data set. Three candidate convolutional neural networks are proposed and the structural parameters of neural networks are provided in Table 2. In which, CNN1 and CNN2 are the same in personalized model Section 5.2, and, in CNN3, Conv3 is the convolutional layer with

Table 1
Structural parameters of personalized neural networks.

Model	No. of Conv	Conv Layer	Pooling Layer	FC Layer
CNN1	1	Conv1	Pool 2×2	128
CNN2	2	Conv1		256
		Conv2	Pool 2×2	64

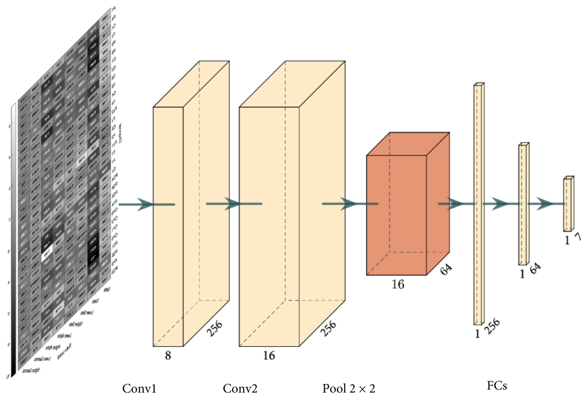

Fig. 10. Personalized CNN.

Table 2
Structural parameters of generalized neural networks.

Model	No. of Conv	Conv Layer	Pooling Layer	FC Layer
CNN1	1	Conv1	Pool 2 × 2	128
CNN2	2	Conv1		256
		Conv2	Pool 2 × 2	64
CNN3	3	Conv1		
		Conv2		256
		Conv3	Pool 2 × 2	64

16 input channels and 32 output channels which is added between the Conv2 and the pooling layer.

5.4. Results

All the models were written in Python 3.7 and PyTorch 1.2.0 and run on a PC with the Intel(R) Core(TM) i7-7700 K CPU @ 4.20 GHz, 32 GB Memory, and NVIDIA GeForce GTX 1080. Two metrics are introduced in the following analysis, accuracy and training time. Accuracy is defined as the percentage of the accurately classified data in the test set, and the training time measures the time consumption for the neural network to be trained. In the following results, the accuracy and training time are calculated by averaging the results from the 10-fold cross validation. We are interested in comparing the ML training speed because, in practice, before entering the fire ground, the previously trained model needs to be updated by new data sets to ensure that it fits the current situation of the firefighter. Thus, the training and implementation of the proposed model can occur simultaneously, i.e., online learning. However, because of some limitations, offline learning is used in this article. In our model, the accuracy and training speed are the metrics in comparing different structures of CNNs. The rationale for using offline learning is further discussed in Section 7.

First, the performance of the two personalized models are compared. According to the training time in Fig. 11, the CNN1 model takes 2.61 s less per iteration to train because of the smaller number of convolutional layers in the structure. The mean accuracy of CNN1 and CNN2 is 94.41% and 94.15%, respectively. Additionally, according to the ANOVA test (F-value: 0.069, p-value: 0.742), the overall accuracy shows no significant differences between CNN1 and CNN2 in Fig. 12. The confusion matrices of the testing result in Figs. 13 and 14 provide detailed information about the classification result given by two personalized models. The classification accuracy of two CNNs are high and less than 5% of samples are unable to be classified between memorizing and performing with the same type of information. Thus, both convolutional neural networks suffice the needs to build a personalized model and classify brain states during the wayfinding task.

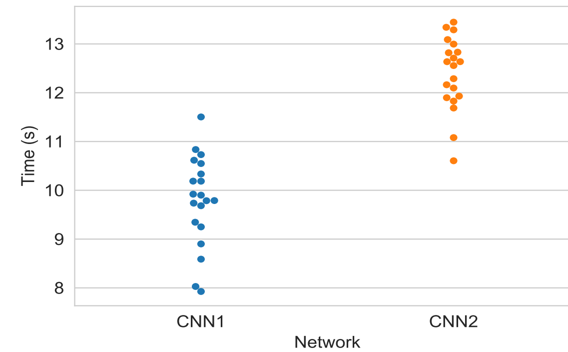

Fig. 11. Personalized neural network training time.

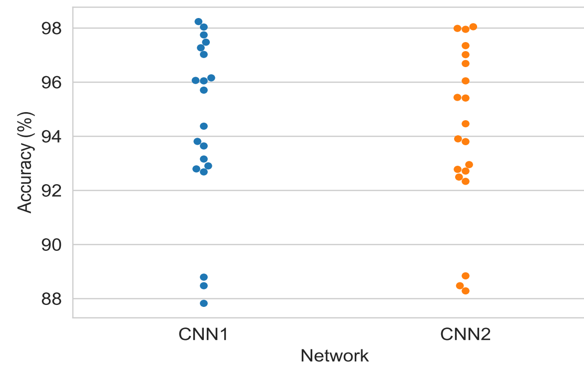

Fig. 12. Personalized neural network overall accuracy.

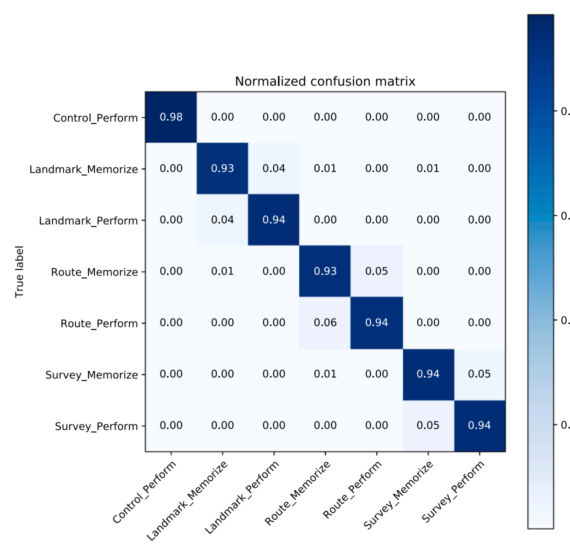

Fig. 13. Confusion matrix of the classification result of CNN1.

However, CNN1 is sufficient for the target and more economical in time and memory requirements.

We used two data sets to test the generalized model. The first one is the 10% remaining data from all the 19 subjects and the remaining one subject is the second data set for testing. As is shown in Fig. 15, the training time for CNN2 is 5.82 s longer than CNN1 on average and the ANOVA test shows that the difference in training time for CNN1 and CNN2 is significant (F-value: 6.36, p-value:0.015). The average training time for CNN3 equals to 293.49 s. It is much longer than the other two networks because of the Conv3 layer. The test on the first data set shows that CNN1 and CNN2 have good results with the average at 69.12% and

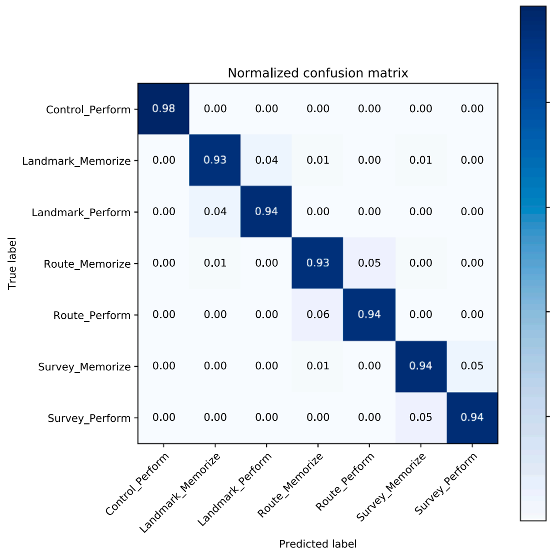

Fig. 14. Confusion matrix of the classification result of CNN2.

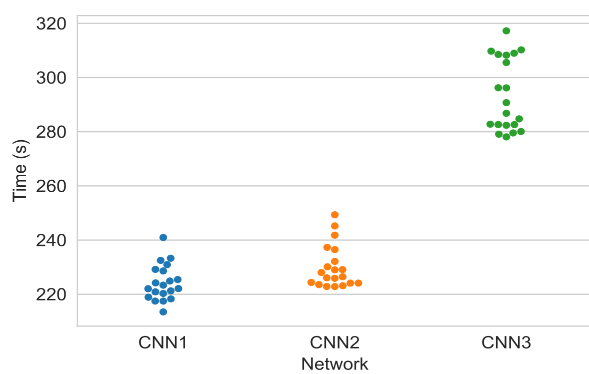

Fig. 15. Generalized neural network training time.

81.22% separately in Fig. 16. Despite relatively high accuracy in some cases, the variance from CNN3 is much higher than those from CNN1 and CNN2. Additionally, none of the convolutional neural networks provided satisfying accuracy on the second data set.

6. Discussion

In this study, a wayfinding experiment was designed to collect the brain activities of subjects when they were memorizing and using different types of information for the wayfinding tasks in an underground maze. After visualizing the PSD of EEG, we implemented convolutional neural networks to classify human cognitive responses in different wayfinding periods based on the EEG data. The study discovered three findings that greatly contribute to the research on wayfinding. First, according to the analysis of individuals in Section 4, the cognitive response of one subject in learning and recall of different types of information shows differences in Figs. 4–7. The result indicates that the wayfinding experiment proposed in Section 3 stimulated diverse PSD distributions in the brain of the subject, which aligns with the change of capabilities of individuals in dealing with various kinds of information in [10]. It further approves the adequacy of the experiment designed in this study to be the stimuli of the mental workload in the wayfinding tasks.

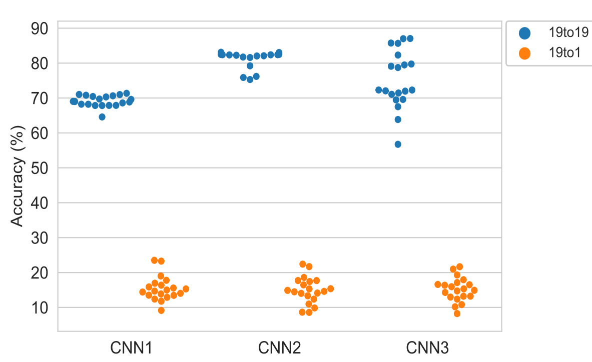

Fig. 16. Generalized neural network overall accuracy.

Second, as discussed in Section 4, even the same information introduced different amounts of mental workload in the same brain region. The observation is coherent with the finding that the same information stimulates different cognitive loads to different people in [10]. Such variation is probably caused by the differences in prior knowledge and intellectual skills. For example, in the control group, some participants follow the right-hand rule. When memorizing the route information, some remembered the first letters of the words, and some encoded the sequence into a rhythm. The finding indicates that the individual difference can be a vital factor that should be considered in building the classification model for EEG signals. Thus, personalized modeling is needed to account for and control the effect brought by individual differences. The need is further validated by the superior classification results of the personalized model comparing generalized models. Additionally, the individual difference is probably introduced by prior knowledge and intellectual skills, and therefore we need robust and efficient (i.e., requiring less data) individual models for trained firefighters.

Third, the personalized classifier based on the PSD and CNN proposed in Section 5.2 has achieved promising performance in detecting the attention of a subject. According to the test result, CNN is proven to be capable of identifying what kind of information the subject is memorizing or recall at high accuracy and a low training time consumption. This neural network structure aligns with the design of CNN in [43,46,47]. Additionally, the success of the CNN1 with the PSD acquired from STFT as the input indicates its potential in identifying the attention of subjects based on the EEG data. It further reveals that the PSD of the EEG signal contains the feature to classify what kind of information the subject is using and whether the subject is memorizing or recall the information. The good performance of CNN1 shows potential applications of CNN as an attention classifier in building the wayfinding information system for firefighters, and in identifying the concentration of subjects and if the subject is encoding or decoding information in the future.

7. Limitations and future work

The study discovered some important findings that can serve as building blocks for future research. We identify the following limitations and point out a few future directions that are worth exploring. First, this study only focused on the PSD of EEG. Other data sets, including the result of the cube comparison test and shape memory test, NASA-TLX questionnaires, the human performance measurements, and other EEG features, such as event-related potentials in [64], have been suggested to provide complementary insights and additional dimensions into understand and quantify cognitive load stimulated by spatial information during the wayfinding experiment. Second, data from more subjects can be collected to test our model, especially provide more insights into the feasibility and validity of generalized models. It is, however, worth noting that there are abundant literature advocates individual differences in capabilities in information processing [10,65,66]. Third, in practice, CNN is required to be updated regularly and before entering the fire ground to eliminate the impact from the changes in prior knowledge and intellectual skills on individuals over time. However, in this study, we are focusing on finding a proper structure of CNN in capturing the mental workload pattern in different scenarios. We will need larger data sets from individuals in multiple experiments over a long period of time to support and validate online learning models. As a result, offline learning is used in this article and the online learning CNN will be implemented in future studies. Fourth, the selection of CNNs and parameters in the models are based on previous research. In [67], multiple machine learning algorithms have given relatively high accuracy for the multi-class classification based on the PSD of EEG data collected in the shape-analogous letter perception experiment. Future studies should test the feasibility of these models as well.

8. Conclusion

Disorientation has been a severe threat to firefighters' safety and lives. Although the advance in information and sensing technologies promises improved wayfinding performances, they can overwhelm firefighters with excessive and varying types of information. The uncertainty of new technologies calls for a better understanding of the connection between the types and format of wayfinding information and its influence on the cognitive load of individuals. This study takes one of the first steps to examine such a connection between stimuli of information and brain activities in wayfinding tasks. Our findings show that memorizing and recall of different types of information stimulate different brain activities. Therefore, personalized models are needed to capture individual brain activity patterns. Our CNN models also indicate that personalized, rather than generalized, models can function as the appropriate attention classifier and thus can serve as the foundation for building the wayfinding systems for firefighters in the future.

Declaration of Competing Interest

The authors declare that they have no known competing financial interests or personal relationships that could have appeared to influence the work reported in this paper.

Acknowledgements

This material is supported by the National Science Foundation (NSF) under Grant Nos. 1937878 and 1761950, as well as the National Institute of Standards and Technology (NIST) under Grant No. 60NANB18D152. Any opinions, findings, and conclusions or recommendations expressed in this material are those of the authors and do not necessarily reflect the views of the National Science Foundation and the National Institute of Standards and Technology.

Appendix A. Supplementary material

Supplementary data associated with this article can be found, in the online version, at https://doi.org/10.1016/j.aei.2020.101180.

References

[1] Z. Roja, V. Kalkis, H. Kalkis, I. Pencis, Assessment of firefighters-rescuers' work severity in relation with interaction between physical and mental load, Proc. Latvian Acad. Sci. Sect. B. Nat. Exact Appl. Sci. 63 (6) (2009) 264–270.
[2] S.N. Henderson, V.B. Van Hasselt, T.J. LeDuc, J. Couwels, Firefighter suicide: understanding cultural challenges for mental health professionals, Profess. Psychol.: Res. Pract. 47 (3) (2016) 224.
[3] B. Evarts, J.L. Molis, United states firefighter injuries 2017, National Fire Protection Association.
[4] C. Brennan, The combat position: Achieving firefighter readiness, Fire Eng. Books (2011).
[5] W.R. Mora, US Firefighter Disorientation Study: 1979-2001, San Antonio, TX, 2003.
[6] R. Zhu, J. Lin, B. Becerik-Gerber, N. Li, Human-building-emergency interactions and their impact on emergency response performance: a review of the state of the art, Saf. Sci. 127 (2020) 104691.
[7] T. Jin, T. Yamada, Experimental study of human behavior in smoke filled corridors, Fire Saf. Sci. 2 (1989) 511–519.
[8] Y. Fang, Y.K. Cho, S. Zhang, E. Perez, Case study of bim and cloud–enabled real-time rfid indoor localization for construction management applications, J. Construct. Eng. Manage. 142 (7) (2016) 05016003.
[9] G. Sallis, D.F. Catherwood, G.K. Edgar, A. Medley, D. Brookes, The human brain in fireground decision-making: trustworthy firefighting equipment? Int. Fire Profess. 5 (2013) 21–24.
[10] J.M. Scandura, Deterministic theorizing in structural learning: three levels of empiricism, J. Struct. Learn. 3 (1) (1971) 21–53.
[11] H. Bhana, Trust but verify, Aero Saf. World 5 (5) (2010) 13–14.
[12] L. Pfeiffer, G. Valtin, N.H. Müller, P. Rosenthal, Aircraft in your head: how air traffic controllers mentally organize air traffic, HUSSO 2015 (2015) 24.
[13] J.M. Wiener, S.J. Büchner, C. Hölscher, Taxonomy of human wayfinding tasks: a knowledge-based approach, Spatial Cognit. Comput. 9 (2) (2009) 152–165.
[14] S. Werner, B. Krieg-Brückner, H.A. Mallot, K. Schweizer, C. Freksa, Spatial cognition: the role of landmark, route, and survey knowledge in human and robot navigation, Informatik'97 Informatik als Innovationsmotor (1997) 41–50.
[15] T.T. Elvins, Visfiles: virtually lost in virtual worlds—wayfinding without a cognitive map, ACM SIGGRAPH Comput. Graph. 31 (3) (1997) 15–17.
[16] A.W. Siegel, S.H. White, The development of spatial representations of large-scale environments, Adv. Child Develop. Behav. 10 (1975) 9–55.
[17] R.G. Golledge, T.R. Smith, J.W. Pellegrino, S. Doherty, S.P. Marshall, A conceptual model and empirical analysis of children's acquisition of spatial knowledge, J. Environ. Psychol. 5 (2) (1985) 125–152.
[18] T. Ishikawa, D.R. Montello, Spatial knowledge acquisition from direct experience in the environment: Individual differences in the development of metric knowledge and the integration of separately learned places, Cognit. Psychol. 52 (2) (2006) 93–129.
[19] P. Jansen, A. Schmelter, M. Heil, Spatial knowledge acquisition in younger and elderly adults, Exp. Psychol. (2009).
[20] A.E. Richardson, D.R. Montello, M. Hegarty, Spatial knowledge acquisition from maps and from navigation in real and virtual environments, Memory Cognit. 27 (4) (1999) 741–750.
[21] P.W. Thorndyke, B. Hayes-Roth, Differences in spatial knowledge acquired from maps and navigation, Cognit. Psychol. 14 (4) (1982) 560–589.
[22] A. Verghote, S. Al-Haddad, P. Goodrum, S. Van Emelen, The effects of information format and spatial cognition on individual wayfinding performance, Buildings 9 (2) (2019) 29.
[23] A. Bosco, L. Picucci, A.O. Caffo, G.E. Lancioni, V. Gyselinck, Assessing human reorientation ability inside virtual reality environments: the effects of retention interval and landmark characteristics, Cognit. Process. 9 (4) (2008) 299–309.
[24] J. Lin, L. Cao, N. Li, How the completeness of spatial knowledge influences the evacuation behavior of passengers in metro stations: a vr-based experimental study, Automat. Construct. 113 (2020) 103136.
[25] J. Lin, L. Cao, N. Li, Assessing the influence of repeated exposures and mental stress on human wayfinding performance in indoor environments using virtual reality technology, Adv. Eng. Informatics 39 (2019) 53–61.
[26] F. Meng, W. Zhang, Way-finding during a fire emergency: an experimental study in a virtual environment, Ergonomics 57 (6) (2014) 816–827.
[27] J. Lin, R. Zhu, N. Li, B. Becerik-Gerber, Do people follow the crowd in building emergency evacuation? a cross-cultural immersive virtual reality-based study, Adv. Eng. Informatics 43 (2020) 101040.
[28] Z. Feng, V.A. González, M. Trotter, M. Spearpoint, J. Thomas, D. Ellis, R. Lovreglio, How people make decisions during earthquakes and post-earthquake evacuation: using verbal protocol analysis in immersive virtual reality, Saf. Sci. 129 (2020) 104837.
[29] T. Hartley, E.A. Maguire, H.J. Spiers, N. Burgess, The well-worn route and the path less traveled: distinct neural bases of route following and wayfinding in humans, Neuron 37 (5) (2003) 877–888.
[30] Y. Shi, J. Du, E. Ragan, Review visual attention and spatial memory in building inspection: toward a cognition-driven information system, Adv. Eng. Informatics 44 (2020) 101061.
[31] Y. Roy, H. Banville, I. Albuquerque, A. Gramfort, T.H. Falk, J. Faubert, Deep learning-based electroencephalography analysis: a systematic review, J. Neural Eng. (2019).
[32] B. He, A. Sohrabpour, E. Brown, Z. Liu, Electrophysiological source imaging: a noninvasive window to brain dynamics, Annu. Rev. Biomed. Eng. 20 (2018) 171–196.
[33] B.T. Jap, S. Lal, P. Fischer, E. Bekiaris, Using eeg spectral components to assess algorithms for detecting fatigue, Expert Syst. Appl. 36 (2) (2009) 2352–2359.
[34] C. Berka, D. Levendowski, M. Lumicao, A. Yau, G. Davis, V. Zivkovic, R. Olmstead, P. Tremoulet, P. Craven, Eeg correlates of task engagement and mental workload in vigilance, learning, and memory tasks, Aviation Space Environ. Med. 78 (5) (2007) B231–B244.
[35] T.O. Zander, C. Kothe, Towards passive brain–computer interfaces: applying brain–computer interface technology to human–machine systems in general, J. Neural Eng. 8 (2) (2011) 025005.
[36] A. Al-Nafjan, M. Hosny, Y. Al-Ohali, A. Al-Wabil, Review and classification of emotion recognition based on eeg brain-computer interface system research: a systematic review, Appl. Sci. 7 (12) (2017) 1239.
[37] F. Lotte, L. Bougrain, M. Clerc, Electroencephalography (eeg)-based brain–computer interfaces, Wiley Encyclopedia Electric. Electron. Eng. (1999) 1–20.
[38] A. Krizhevsky, I. Sutskever, G.E. Hinton, Imagenet classification with deep convolutional neural networks, Adv. Neural Inf. Process. Syst. (2012) 1097–1105.
[39] R. Schirrmeister, J. Springenberg, L. Fiederer, M. Glasstetter, K. Eggensperger, M. Tangermann, F. Hutter, W. Burgard, T. Ball, Deep learning with convolutional

neural networks for eeg decoding and visualization, Hum. Brain Mapping 38 (11) (2017) 5391–5420.
[40] I. Ullah, M. Hussain, H. Aboalsamh, An automated system for epilepsy detection using eeg brain signals based on deep learning approach, Expert Syst. Appl. 107 (2018) 61–71.
[41] L. Chu, R. Qiu, H. Liu, Z. Ling, T. Zhang, J. Wang, Individual recognition in schizophrenia using deep learning methods with random forest and voting classifiers: Insights from resting state eeg streams, arXiv preprint arXiv: 1707.03467.
[42] M. Hajinoroozi, Z. Mao, T.P. Jung, C.T. Lin, Y. Huang, Eeg-based prediction of driver's cognitive performance by deep convolutional neural network, Signal Process.: Image Commun. 47 (2016) 549–555.
[43] J. Zhang, S. Li, R. Wang, Pattern recognition of momentary mental workload based on multi-channel electrophysiological data and ensemble convolutional neural networks, Front. Neurosci. 11 (2017) 310.
[44] D.F. Wulsin, J.R. Gupta, R. Mani, J.A. Blanco, B. Litt, Modeling electroencephalography waveforms with semi-supervised deep belief nets: fast classification and anomaly measurement, J. Neural Eng. 8 (3) (2011) 036015.
[45] I. Sturm, S. Lapuschkin, W. Samek, K.R. Müller, Interpretable deep neural networks for single-trial eeg classification, J. Neurosci. Meth. 274 (2016) 141–145.
[46] N.D. Truong, A.D. Nguyen, L. Kuhlmann, M.R. Bonyadi, J. Yang, S. Ippolito, O. Kavehei, Convolutional neural networks for seizure prediction using intracranial and scalp electroencephalogram, Neural Netw. 105 (2018) 104–111.
[47] J. Teo, C.L. Hou, J. Mountstephens, Preference classification using electroencephalography (eeg) and deep learning, J. Telecommun. Electron. Comput. Eng. (JTEC) 10 (1–11) (2018) 87–91.
[48] Unity, Maze generator, https://assetstore.unity.com/packages/tools/modeling/maze-generator-41853, 2019.
[49] R.B. Ekstrom, D. Dermen, H.H. Harman, Manual for kit of factor-referenced cognitive tests, vol. 102, Educational testing service, Princeton, NJ, 1976.
[50] A. Motamedi, Z. Wang, N. Yabuki, T. Fukuda, T. Michikawa, Signage visibility analysis and optimization system using bim-enabled virtual reality (vr) environments, Adv. Eng. Informatics 32 (2017) 248–262.
[51] A. Delorme, S. Makeig, Eeglab: an open source toolbox for analysis of single-trial eeg dynamics including independent component analysis, J. Neurosci. Meth. 134 (1) (2004) 9–21.
[52] N. Bigdely-Shamlo, T. Mullen, C. Kothe, K.M. Su, K.A. Robbins, The prep pipeline: standardized preprocessing for large-scale eeg analysis, Front. Neuroinformatics 9 (2015) 16.
[53] J. Onton, S. Makeig, Information-based modeling of event-related brain dynamics, Progr. Brain Res. 159 (2006) 99–120.
[54] A. Mognon, J. Jovicich, L. Bruzzone, M. Buiatti, Adjust: An automatic eeg artifact detector based on the joint use of spatial and temporal features, Psychophysiology 48 (2) (2011) 229–240.
[55] P. Mirowski, D. Madhavan, Y. LeCun, R. Kuzniecky, Classification of patterns of eeg synchronization for seizure prediction, Clin. Neurophysiol. 120 (11) (2009) 1927–1940.
[56] A. Fink, R.H. Grabner, C. Neuper, A.C. Neubauer, Eeg alpha band dissociation with increasing task demands. cognitive brain research, Cognit. Brain Res. 24 (2) (2005) 252–259.
[57] R. Cabeza, L. Nyberg, Imaging cognition ii: An empirical review of 275 pet and fmri studies, J. Cognit. Neurosci. 12 (1) (2000) 1–47.
[58] P. Sauseng, W. Klimesch, M. Schabus, M. Doppelmayr, Fronto-parietal eeg coherence in theta and upper alpha reflect central executive functions of working memory, Int. J. Psychophysiol. 57 (2) (2005) 97–103.
[59] P. Sauseng, W. Klimesch, M. Doppelmayr, S. Hanslmayr, M. Schabus, W.R. Gruber, Theta coupling in the human electroencephalogram during a working memory task, Neurosci. Lett. 354 (2) (2004) 123–126.
[60] D. Sridharan, D.J. Levitin, V. Menon, A critical role for the right fronto-insular cortex in switching between central-executive and default-mode networks, Proc. Natl. Acad. Sci. 105 (34) (2008) 12569–12574.
[61] E.J. Hwang, M. Hauschild, M. Wilke, R.A. Andersen, Inactivation of the parietal reach region causes optic ataxia, impairing reaches but not saccades, Neuron 76 (5) (2012) 1021–1029.
[62] R. Elliott, Executive functions and their disorders: Imaging in clinical neuroscience, Br. Med. Bull. 65 (1) (2003) 49–59.
[63] D.P. Kingma, J. Ba, Adam: A method for stochastic optimization, arXiv preprint arXiv:1412.6980.
[64] M. Tlauka, C.R. Clark, P. Liu, M. Conway, Encoding modality and spatial memory retrieval, Brain Cognit. 70 (1) (2009) 116–122.
[65] M.S. Humphreys, W. Revelle, Personality, motivation, and performance: a theory of the relationship between individual differences and information processing, Psychol. Rev. 91 (2) (1984) 153.
[66] M.E. Faust, D.A. Balota, D.H. Spieler, F.R. Ferraro, Individual differences in information-processing rate and amount: implications for group differences in response latency, Psychol. Bull. 125 (6) (1999) 777.
[67] R. Bose, S.K. Goh, K.F. Wong, N. Thakor, A. Bezerianos, J. Li, Classification of brain signal (eeg) induced by shape-analogous letter perception, Adv. Eng. Informatics 42 (2019) 100992.